RSC Advances

PAPER

View Article Online
View Journal | View Issue



Cite this: *RSC Adv.*, 2015, **5**, 76451

# Large-scale production of ureido-cytosine based supramolecular polymers with well-controlled hierarchical nanostructures†

Chih-Chia Cheng,*[a] Feng-Chih Chang,[b] Jui-Hsu Wang,[b] Yu-Lin Chu,[b] Yeh-Sheng Wang,[b] Duu-Jong Lee,[cd] Wei-Tsung Chuang[e] and Zhong Xin[f]

Received 7th August 2015
Accepted 3rd September 2015

DOI: 10.1039/c5ra15849d

www.rsc.org/advances

A novel supramolecular polymer containing urea-cytosine (UrCy) quadruple hydrogen-bonding moieties that possesses a high association constant ($K_a$ > $10^6$ $M^{-1}$) was synthesized at high yield (96%) at kilogram-scale. The synthesized telechelic macromer dissolved in solution can undergo a substantial change in solution viscoelasticity and can self-assemble due to the noncovalent nature of supramolecular polymerization. As the concentration of UrCy in solution was increased, the spherical assemblies gradually transformed to an ordered lamellar phase with an extremely high degree of polymerization. In addition, the dynamic behavior of UrCy units induced a sudden phase transition in the bulk state, revealing an interesting order–disorder transition from a crystalline solid to liquid state. This newly-discovered material has excellent polymer-like features that are distinct to existing systems. A simple path for forming supramolecular polymers is recommended for the design, large-scale production and manipulation of self-assembled materials with distinctive properties.

## Introduction

Organic polymers based on supramolecular assemblies as building blocks have attracted much research attention. Fabrication of molecular objects can be manipulated through cooperative non-covalent interactions of atomic bonds, including hydrogen bonding, ionic interactions, metal coordination, electrostatic interactions and π–π stacking;[1] by doing so, materials with novel properties can be obtained, such as highly-specific chemical and physical properties and spontaneous self-assembly behavior.[2,3] Improved reversibility in the bonding between the monomer units of novel materials was established by achieving supramolecular polymerization.[4,5] For instance, the base pairing properties of nucleobase-functionalized materials can be improved by introducing complementary hydrogen bonds in a reversible non-covalent matrix to construct a three-dimensional structure.[6,7] Biomolecular structures constructed using different types of hydrogen bonding modules have been proposed to bind as building blocks to achieve the required qualities in supramolecular polymers.[3]

The process of hydrogen-bonding supramolecular assembly into multicomponent structures can be refined, as the strength of the hydrogen bonds can be easily tuned by altering the donor (D) and acceptor (A) sites to obtain the desired functional structures without using covalent polymerization. Kolomiets and Lehn,[8] Binder *et al.*[9] and Würthner *et al.*[10] used the hydrogen bonding motif to prepare chain-extended supramolecular polymers, which underwent assembly *via* a strong Hamilton–barbituric acid interaction. Zimmerman and coworkers[11] used quadruple hydrogen-bonded ureidodeazapterin motif in combination for the preparation of hexameric aggregates and supramolecular polymers. Meijer and co-workers[12,13] developed a series of functionalized supramolecular polymers with association constants ($K_a$) up to $10^7$ $M^{-1}$ based on quadruple hydrogen bonding ureido-pyrimidinone (UPy) moieties. Incorporation of self-complementary UPy units into polymers results in a spontaneous increase in molecular weight and improves the mechanical properties of polymers. Hailes and co-workers[14] developed a new family of quadruple hydrogen-bonding modules based on a cytosine derivative. Ureido-substituted cytosine (UrCy) is presented in a DDAA arrangement of hydrogen-bonding groups with a high $K_a$ ($9 \times 10^6$ $M^{-1}$ in deuterated benzene), and can only freely rotate

[a]*Graduate Institute of Applied Science and Technology, National Taiwan University of Science and Technology, Taipei 10607, Taiwan. E-mail: cccheng@mail.ntust.edu.tw; Fax: +886-2-27303733; Tel: +886-2-27303747*

[b]*Institute of Applied Chemistry, National Chiao Tung University, Hsin Chu 30050, Taiwan*

[c]*Department of Chemical Engineering, National Taiwan University, Taipei 10617, Taiwan*

[d]*Department of Chemical Engineering, National Taiwan University of Science and Technology, Taipei 10607, Taiwan*

[e]*National Synchrotron Radiation Research Center, Hsinchu 30076, Taiwan*

[f]*State Key Laboratory of Chemical Engineering, School of Chemical Engineering, East China University of Science and Technology, Shanghai 200237, China*

† Electronic supplementary information (ESI) available: Experimental part including synthesis procedures, structural characterizations, variable-temperature XRD and related data. See DOI: 10.1039/c5ra15849d

around the amide bond preventing conformational changes. In addition, the involved UrCy groups are located in separate oligomer chain ends, allowing formation of a supramolecular polymer without initiating covalent polymerization.[15] Nevertheless, it remains challenging to identify synthetic routes suitable for the large-scale production of supramolecular polymers.

A series of pyrimidine-functionalized polymers (PFP) that exhibit interesting viscoelastic, self-assembly and photoelectronic properties have been developed.[16–22] For example, incorporation of pyrimidine bases (uracil and thymine) into different polymer systems was shown to produce polystyrene,[16,17] poly(ε-caprolactone),[18] polybenzoxaine[19] and conjugated polymers.[20–22] The pyrimidine complex plays a very important role in the processes of photosensitization and light emission, which can be fabricated into organic light-emitting devices with a high hole-transporting ability.[21,22] These materials can also be transformed into covalent network structures through exposure to UV light at a wavelength of 254 nm.[17] Based on these principles, this study extended the application of PFP to UrCy-based supramolecular polymer synthesis by proposing a simple pathway for the large-scale production of a UrCy-end-capped polypropylene glycol derivative (UrCy–PPG) using commercially-available chemicals. We demonstrate that this novel material can spontaneously self-assemble into a higher-level structure as a result of the incorporation of self-complementary hydrogen bonding interactions, and behaves as a polymer in both the solution and bulk states. A sudden phase transition in UrCy–PPG is observed in the bulk state, which represents an excellent thermoreversible property that allows the mechanical and viscoelastic properties to be restored at ambient temperature.

## Experimental section

A difunctional Cy-PPG was prepared by Michael addition of PPG diacrylate to cytosine. UrCy–PPG was prepared by isocyanate chemistry of Cy-PPG in the presence of *n*-butylisocyanate. The samples for transmission electron microscopy (TEM) and scanning electron microscope (SEM) investigations were prepared by placing a drop of the sample solution onto a glass substrate and then evaporating the solvent (toluene). Variable temperature X-ray diffraction (XRD) and rheological analyses were performed at a heating/cooling rate of 3 °C $min^{-1}$ in an air atmosphere. The general materials and instrumentation used in this work are described in more detail in the ESI.†

### Syntheses

**(1) Synthesis of cytosine-terminated PPG (Cy-PPG).** Poly(propylene glycol) diacrylate 800 (1050 g, 1.312 mol), cytosine (307 g, 2.760 mol) and sodium *t*-butoxide (0.3 g, 0.003 mol) were solved in 1000 mL of dimethyl sulfoxide (DMSO) in a flask and the reaction mixture was stirred at 60 °C for 48 h. After evaporation of the solvent, the crude product was redissolved in toluene (500 mL) and insoluble impurities were removed by hot filtration. Finally, the toluene was evaporated, and then the product was dried under a vacuum. Yield: 97% (1298 g).

**(2) Synthesis of UrCy–PPG.** Cy-PPG (1048 g, 1.025 mol) was dissolved in dry chloroform (1000 mL), cooling down to 5 °C in an ice bath. *n*-Butylisocyanate (214 g, 2.155 mol) was injected dropwise through a syringe over a period of 1 h while the reaction mixture was stirred at 5 °C for 2 h. Then the product was placed at ambient temperature for an additional 24 h. Eventually, the reaction mixture was filtered and the solvent was evaporated. The residue was purified by precipitation in diethyl ether. Yield: 95% (1118 g).

## Results and discussion

### Synthesis and self-complementary behavior of the UrCy telechelic supramolecular polymer

A novel, well-defined, end-functional UrCy polymer created *via* a simple two-step synthesis was developed in this study, as shown in Scheme S1.† The polymer has a self-complementary arrangement owing to the strongly hydrogen-bonded UrCy–UrCy pairs. Polypropylene glycol (PPG) was chosen as the polymer backbone as it is widely used in surfactants, drug carriers and elastomer products. A low molecular weight oligomer, cytosine-terminated PPG (Cy-PPG), was obtained by Michael addition of poly(propylene glycol) diacrylate 800 (PPG diacrylate, *ca.* 14 repeat units) to cytosine. The final product was produced *via* an isocyanate-mediated reaction with Cy-PPG, allowing the preparation of supramolecular UrCy–PPG, which possesses quadruple hydrogen bonding units at the polymer ends. This innovative approach successfully produced significant quantities (kilogram-scale) of supramolecular polymers with a high-yield (96%). The structural formula for UrCy–PPG is shown in Scheme 1a. In order to investigate the stability of the hydrogen bonding interaction in the UrCy–PPG system, variable-temperature NMR experiments were performed in toluene-*d*8 solutions of UrCy–PPG (shown in Fig. S3†). At 25 °C, two characteristic peaks of both urea N–H protons (10.91 and 9.50 ppm), corresponding to the formation of a hydrogen bonding interaction between UrCy functional groups, were observed. When the UrCy–PPG solution was heated from 25 °C to 100 °C, the peaks at 10.91 and 9.50 ppm shifted slightly upfield to 10.53 and 9.15 ppm, respectively. This observation shows that temperature only had a minor effect on the dynamic interactions between UrCy functional groups, mainly due to the influences of the self-complementary hydrogen bonds and presence of cyclic species[23] (Scheme 1b). Furthermore, concentration-dependent NMR studies were carried out in order to assess the binding affinity of UrCy–PPG, as presented in Fig. S4.† Surprisingly, no significant changes in the chemical shift occurred over a wide range of concentrations (from 0.00165 to 0.25 g $mL^{-1}$) in toluene-*d*8, suggesting that self-complementary dimerization of UrCy–PPG occurs rapidly (on the NMR time-scale) to form extremely stable hydrogen-bonded complexes in toluene. Accordingly, this aroused interest in investigating the self-assembly of UrCy–PPG in solution.

 

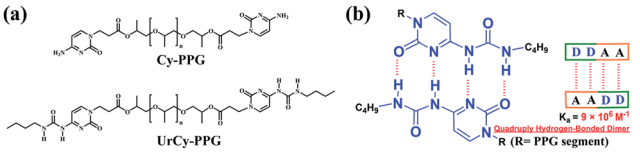


Scheme 1 (a) Chemical structures of Cy-PPG and UrCy–PPG. (b) Representative structure of the hydrogen-bonded UrCy dimer.

## Self-assembly and polymer-like behavior of UrCy–PPG in solution

In order to evaluate the effects of the hydrogen bonding complexes in solution, the assembly behavior of UrCy–PPG was investigated using the Ubbelohde viscometer and diffusion-ordered NMR spectroscopy (DOSY). All experiments were carried out in toluene in order to avoid interactions between a polar solvent and the supramolecular functional groups.[24] The concentration-dependent viscosities of UrCy–PPG, Cy-PPG and PPG diacrylate are shown in Fig. 1a. No remarkable increase in viscosity was observed at concentrations below 0.035 g $mL^{-1}$ for any test sample, implying that significant polymer chain entanglement effects did not occur due to dilution. However, when the solution concentration exceeded a critical value (0.035 g $mL^{-1}$), the viscosity of UrCy–PPG dramatically increased compared to Cy-PPG and PPG diacrylate, as shown in Fig. 1a. This suggests significantly greater formation of hydrogen bonding interactions between individual UrCy–PPG monomer units compared to Cy-PPG and PPG diacrylate monomer units, even though Cy-PPG contains cytosine groups coupled to the ends of the polymer chain. Further diffusion coefficient measurements for UrCy–PPG in toluene-*d*8 provided evidence of the influence of viscosity on the extended hydrogen-bonded supramolecular polymers. These experiments were carried out by analyzing the degree of polymerization (DP) over the concentration range from 0.03 g $mL^{-1}$ to 0.25 g $mL^{-1}$. All diffusion coefficients were strongly dependent on concentration (Fig. 1b). At a concentration of 0.03 g $mL^{-1}$, the diffusion coefficient was calculated to be $4.38 \times 10^{-10}$ $m^2$ $s^{-1}$, indicating the presence of oligomeric forms under a low DP in dilute toluene solutions.[10,23c] Upon further increasing the UrCy–PPG concentration to 0.25 g $mL^{-1}$, the diffusion coefficient decreased linearly to $7.88 \times 10^{-11}$ $m^2$ $s^{-1}$. In addition, construction of the extended supramolecular structure was assessed *via* DOSY experiments using DP values of up to approximately 315 at a concentration of 0.25 g $mL^{-1}$ at 25 °C (for further details see the ESI†). It has been suggested that supramolecular polymers grow significantly in high concentrations of toluene due to the presence of UrCy end-groups. This phenomenon results in concentration-dependent self-assembly of supramolecular polymerization.[25] In order to confirm the results described above, the growth processes of self-assembled nanostructures were observed using TEM. Test samples were prepared by dropping different concentrations of UrCy–PPG toluene solutions onto separate carbon-coated copper grids. At a concentration of 0.03 g $mL^{-1}$ (Fig. 1c), TEM revealed the phenomena of self-assembly into a particle-like morphology with a diameter of 7–10 nm. This implies that the UrCy–PPG particles can cluster to form cyclic oligomers *via* intramolecular chain-stacking and the UrCy hydrogen bonding interactions (Scheme S2†).[25] When the concentration of UrCy–PPG was increased to 0.075 g $mL^{-1}$ (Fig. 1f), aggregates with disordered, branch-like fibers appeared to be associated with local particles, which can attributed to the phenomenon of viscous drag (Fig. 1a). When the concentration just exceeded 0.25 g $mL^{-1}$, well-ordered lamellar structures could be observed, as shown in Fig. 1g. The dark region corresponds to the UrCy segment while the bright region belongs to the PPG segment. The lamellar spacing between UrCy and PPG segments can be controlled down to the nanoscale range, suggesting that the nanostructures are neatly arranged to form lamellar patterns, organized through hierarchical growth of the branch-like fibers. These results provided good agreement with the viscosity and DOSY analyses (Fig. 1a and b). It should be noted that the concentration-induced phase transition results in a lamellar ordered state when the equilibrium state was reached. This is in contrast to previous reports addressing the host structure of supramolecular polymers that form fibrous structures.[23c,26]

Fig. 1h presents further evidence to demonstrate that a self-organization mechanism predicts the transition from particle aggregation to a lamellar phase as the concentration ratio of UrCy–PPG increased. The formation of zero-dimensional nanoparticles at very dilute concentrations is attributable to environmental effects, as the cyclic oligomers are too short to hinder the formation of chain entanglements. Thus, clusters of cyclic oligomers piled up to form a micellar aggregation associated with the formation of small particles (Fig. 1h and Scheme S2†). On the contrary, lamellar patterns were formed at high

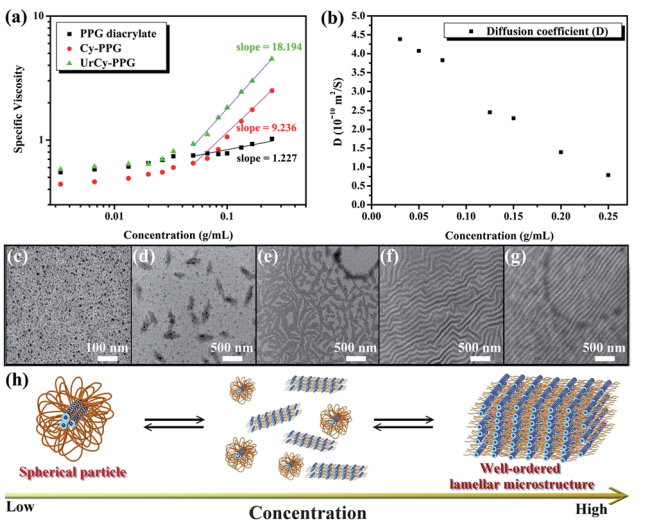


Fig. 1 Spontaneous formation of polymer-like features in toluene solution. (a) Plot of specific viscosity *versus* concentration in toluene at 25 °C for various polymers. (b) Plot of diffusion coefficient as a function of concentration for supramolecular polymerization of UrCy–PPG. TEM images of UrCy–PPG on carbon-coated copper grids at different concentrations: (c) 0.03, (d) 0.05, (e) 0.075, (f) 0.2 and (g) 0.35 g $mL^{-1}$. (h) Graphical representation of the hierarchical self-assembly of UrCy–PPG in solution.

concentrations – presumably from cyclic and linear oligomers combing into a form of parallel stripes (Fig. 1h and Scheme S2†). This created linear arrays of supramolecular polymers with a high DP. These results also demonstrate the feasibility and utility of UrCy modules for inducing morphological changes in polymeric self-assembly systems.

### Hierarchical organization of thermoresponsive supramolecular polymers in the bulk state

Supramolecular assembly can be used to control the nanoarchitecture of a polymeric matrix; by doing so, unique physical properties can be generated in the matrix.[6] Fig. 2a presents the DSC thermal curves for UrCy–PPG, Cy-PPG and PPG diacrylate. UrCy–PPG exhibited a melting point ($T_m$) of 100.2 °C and a clear glass transition temperature ($T_g$) of −47.8 °C, whereas Cy-PPG and PPG diacrylate only underwent $T_g$ at −19.5 °C and −69.4 °C, respectively. This implies that connection of UrCy units to the PPG chain ends results in enhanced packing of its molecular chains. Therefore, self-complementary and non-complementary stickers result in very different mesoscopic arrangements and a significant change in macroscopic properties. When the stickers are non-complementary pairs and self-complementary pairs, respectively, Cy-PPG and PPG diacrylate behave as a viscous liquid (Fig. 2b and c) whereas UrCy–PPG appears as a translucent yellow-colored, firm, elastic film (Fig. 2d and e). The polarized optical microscopy images presented in Fig. S5† show that the crystal morphology revealed a spherulite-like "Maltese-cross" pattern in UrCy–PPG thin film. Based on these observations, crystallinity only affects the UrCy moieties, while the PPG segment remains amorphous in format. The strength of the material is gained from close-packing of UrCy end-groups transferring into hard microdomains, which can aid the supramolecular binding motif in the bulk state and play a dominant role in affecting the phase separation between the UrCy and PPG chains.

Variable-temperature Fourier transform infrared (FTIR) experiments were performed to investigate the effect of hydrogen bonding associations on phase separation. Fig. S6† illustrates the N–H stretching region of UrCy–PPG at 30 °C, in which characteristic peaks were observed at frequencies of 3215 and 3177 $cm^{-1}$; typical values for strongly hydrogen-bonded N–H.[27] This demonstrates that the UrCy interactions provide highly directional and self-complementary bonding. The effect of temperature was also investigated by increasing the temperature from 30 °C to 120 °C; the medium hydrogen-bonded N–H peak shifted slightly to a higher wave number around 3243 $cm^{-1}$. This finding indicates that heating minimally affected the hydrogen bonding interaction of the UrCy–PPG stickers and that UrCy–PPG forms highly-stable hydrogen-bonded complexes in the solid state. In the lower wave number region (1600–1800 $cm^{-1}$) of the FTIR spectra (Fig. S6†), four carbonyl stretching peaks were observed at 30 °C; these peaks at 1729, 1705, 1657 and 1618 $cm^{-1}$ correspond to the contributions of amorphous, crystalline ester–carbonyl stretching, hydrogen-bonded urea and strongly-associated UrCy carbonyl groups, respectively. When the temperature was increased from 30 °C to 120 °C, two new peaks at 1626 and 1682 $cm^{-1}$ appeared, along with disappearance of the 1618 $cm^{-1}$ peak; these changes could be explained by rapid destruction of the hydrogen bonding interactions of the cytosine ring. Surprisingly, the peak of hydrogen-bonded urea carbonyl group was slightly shifted to lower wavenumbers (from 1657 to 1651 $cm^{-1}$). This observation indicates that the hydrogen bonding interaction of urea group remains almost unchanged during heating and melting is not associated with disruption of the urea hydrogen bonds. However, when the temperature was above 100 °C, the amorphous ester–carbonyl band at 1718 $cm^{-1}$ appeared as the strongly hydrogen-bonded carbonyl groups were destroyed and rearranged, as indicated by the formation of characteristic bands at 1626, 1651 and 1682 $cm^{-1}$ (Fig. S6†). This observation implies that UrCy–PPG begins to melt around 100 °C when the phase transition occurs. Therefore, we can conclude that the crystallization/melting behavior is related to the hydrogen-bonded transition structures within UrCy–PPG.

The relationship between the phase transition and evolution of the microstructure was studied by performing variable-temperature XRD experiments *via* direct observation of the self-assembly process of UrCy–PPG. As shown in Fig. 3a, the XRD profile of UrCy–PPG at 30 °C displayed two reflection peaks at $q$ = 6.40 $nm^{-1}$ ($d$ = 0.98 nm) and $q$ = 7.38 $nm^{-1}$ ($d$ = 0.85 nm). The $d$-spacing of 0.98 nm suggests that the stacks of dimerized UrCy are held together *via* multiple hydrogen-bonding interactions in these interaction domains.[28,29] The spacing of 0.85 nm in the crystal lattice is the distance between the plane of closely-packed UrCy dimers,[30,31] as a result of combining specific structures with a regular structure. Therefore, these stacked arrays display strong positions at $q$ = 7.38, 13.07, 14.54 and 19.37 $nm^{-1}$, corresponding to the close packing of UrCy segments, a consequence of the crystallization of UrCy end groups that tend to align end-to-end with self-assembly into microdomains. In addition, a long-range, well-ordered, self-assembled nanostructure was clearly observed, based on the fact that UrCy–PPG showed highly-ordered lamella microstructures ($q$ = 1 up to 5), with the first intense reflection at $q$ = 0.96 $nm^{-1}$, corresponding to a spacing of $d$ = 6.54 nm. This observed spacing value is significantly higher than the theoretical value of structural units (Scheme 1), which is possibly attributed to the chain alignment and extension of

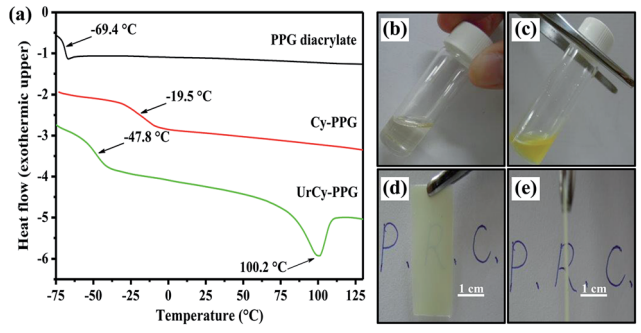


Fig. 2 Characterization of self-assembly behavior in the bulk state. (a) DSC curves for cytosine-functioned PPGs and the controlled PPG diacrylate. Appearance of (b) PPG diacrylate, (c) Cy-PPG and (d and e) UrCy–PPG.

 

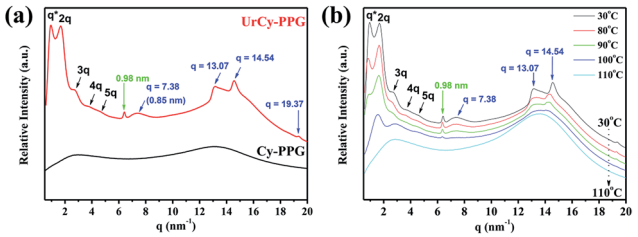


Fig. 3 Long-range ordering of supramolecular polymers induced by complementary interactions. (a) One-dimensional XRD data for Cy-PPG and UrCy–PPG recorded at 30 °C. (b) Variable-temperature XRD data for UrCy–PPG recorded at a range of temperatures from 30 °C to 110 °C at 3 °C $min^{-1}$.

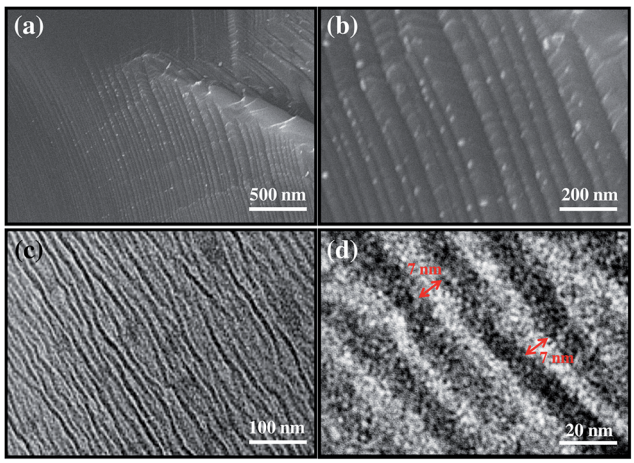


Fig. 4 Controlling the crystalline structure and morphology of UrCy–PPG. SEM (a and b) and TEM (c and d) images showing the lamellar structures of annealed UrCy–PPG; the width of the lamellar structures is indicated by arrows in (d).

flexible PPG segments during the crystallization process. However, the precursor Cy-PPG displayed a typical amorphous structure. This observation indicates that the UrCy–PPG system exhibits a strong phase separation between UrCy and PPG segments, resulting in a stable, confined crystallization in a lamellar arrangement. Furthermore, SEM and TEM experiments were performed to confirm the lamellar structure of UrCy–PPG (Fig. 4). The images suggested that the lamellar structure of the complex was *ca.* 7 nm wide. Similar results were obtained from the XRD data discussed above, in which the UrCy–PPG system exhibited well-ordered lamellar structures. However, as the temperature was increased from 30 °C to 110 °C, a periodic XRD peak was not observed, indicating a long-range ordered structure did not form due to melting of the lamellar phase (Fig. 3b). Conversely, as soon as the sample was cooled to 30 °C, the diffraction pattern spontaneously returned to its original lamellar structure (Fig. S7†). As a result of this restatement, the UrCy end-functionalized hydrogen-bonded supramolecular complexes underwent a thermoreversible transition between disordered liquids and fully-ordered crystalline lamellas. As melting is homogeneous by nature, microphase separation occurs when crystallization and hierarchical self-assembly of the crystallizable phase into the lamellar phases occurred, creating the arrangement of the pliably amorphous segment.[32]

The phase transition was directly observed by carrying out rheological experiments; the results are shown in Fig. 5a. Dynamic storage modulus ($G'$), loss modulus ($G''$) and complex viscosity were plotted against temperature in a double logarithmic format. As the temperature increased above 100 °C, the rheological response of UrCy–PPG underwent a sudden thermal transition from highly elastic ($G' > G''$) to predominantly viscous ($G'' > G'$) behavior. At the same time, the viscosity of UrCy–PPG reduced significantly from $10^5$ Pa s at 98 °C to 10 Pa s at 103 °C. This indicates that the temperature-dependent association between individual monomer units occurs as an interesting order–disorder transition from a crystalline solid to the liquid state when temperature increased, even though UrCy–PPG has an orderly polymer chain arrangement (Fig. 1b and 3a). This orderly arrangement was evidenced by the fact that the hydrogen bonds dissociated and rearranged when temperature increased, suggesting a change in the nature of the hydrogen bond conformation. Rheological data also agreed with the FT-IR results (Fig. S6†). In order to understand the effect of the structural phase transition on thermoreversible stability, a validation of multi-cycle rheological measurements over the temperature range of 50–160 °C was carried out (Fig. 5b). Over multiple heating and cooling cycles, UrCy–PPG appeared to undergo a conspicuous temperature-dependent response and the elastic modulus reverted back perfectly to the original values for each state as the temperature decreased, as a result of the connection between the phase behavior and thermoplastic properties. In a controlled experiment, Cy-PPG displayed the opposite trend under the same experimental conditions (Fig. S8†). These results further confirm the excellent thermoreversible stability of UrCy–PPG, due to the presence of the UrCy end groups and their stable links that maintain the three-dimensional order in the structure.

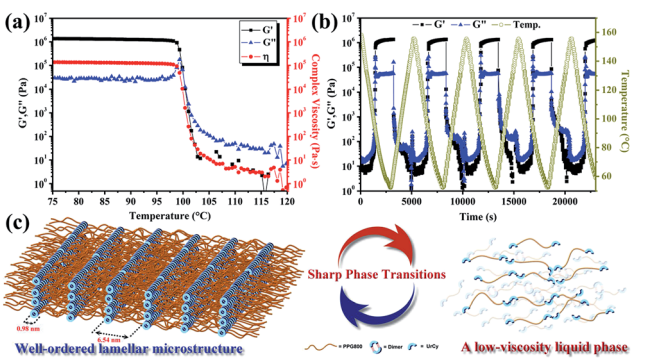


Fig. 5 Effect of the order–disorder transition on the rheological behavior of UrCy–PPG. Rheology data for UrCy–PPG: (a) temperature stability sweep of storage modulus ($G'$), loss modulus ($G''$) and complex viscosity at the temperature range between 75 °C and 120 °C. (b) Temperature cycling rheology experiments for UrCy–PPG: $G'$, $G''$ (solid symbols) and temperature (open symbol) variations *versus* time. (c) Suggested processes for the transition between the lamellar and liquid phases in bulk state.

Over the small temperature range between 100 °C and 103 °C, an order–disorder phase transition resulted in a significant change in UrCy–PPG from a well-ordered lamellar microstructure to a more disordered liquid state (Fig. 5c). Below the transition temperature, the UrCy–PPG self-assembly process proceeded and resulted in an extended polymeric structure, due to the occurrence of supramolecular polymerization contributed by the strongly-associating UrCy functional groups. The close π–π stacking of UrCy dimers forms a crystal lattice, then lamellar-like structures are formed by aggregation of crystals, which behave like multiple hard blocks dispersed within the PPG domains. Note that an incompatibility was observed between the polar hard blocks and hydrophobic PPG segments; this enabled the structure to grow and transfer into a high-performance supramolecular polymer. This implies that the hard domain of UrCy plays a functional role as physical cross-linker, causing the structure to behave a thermoplastic elastomer and form a long-range, directionally-ordered network.

## Conclusions

In summary, a novel UrCy–PPG macromer was developed for the synthesis of high-quality supramolecular polymers in large-scale production (kilogram-scale) utilizing only commercially-available chemicals. The novel macromer exhibits a high dimerization constant, excellent thermoreversible bonding ability and self-assembly properties in both solution and the solid state, as a result of UrCy–induced supramolecular polymerization. The UrCy units incorporated in the PPG chain ends result in microphase separation, dramatically altering the morphologies from spherical to lamellar nanostructures with an extremely high degree of polymerization. In addition, a sudden temperature-induced phase transition was identified. The phase transition is triggered by dynamic interaction between dimerized UrCy moieties, making UrCy–PPG highly attractive for rapid re-bonding/dissociation process. Overall, the present study provides a new and simple path for the large-scale production of supramolecular polymeric materials with excellent self-assembly properties.

## Acknowledgements

We thank the National Synchrotron Radiation Research Center (NSRRC, Taiwan) for their support with the XRD and rheological measurements. This study was financially supported by "Aim for the Top University Plan" of the National Taiwan University of Science and Technology and the Ministry of Science and Technology, Taiwan (contract no. MOST 103-2218-E-011-012).

## Notes and references

1 S. Seiffert and J. Sprakel, *Chem. Soc. Rev.*, 2012, **41**, 909–930.
2 C. R. South, C. Burd and M. Weck, *Acc. Chem. Res.*, 2007, **40**, 63–74.
3 A. J. Wilson, *Soft Matter*, 2007, **3**, 409–425.
4 L. Brunsveld, B. J. B. Folmer, E. W. Meijer and R. P. Sijbesma, *Chem. Rev.*, 2001, **101**, 4071–4097.
5 J. L. Sessler, C. M. Lawrence and J. Jayawickramarajah, *Chem. Soc. Rev.*, 2007, **36**, 314–325.
6 T. Aida, E. W. Meijer and S. I. Stupp, *Science*, 2012, **335**, 813–817.
7 J. L. Sessler and J. Jayawickramarajah, *Chem. Commun.*, 2005, 1939–1949.
8 E. Kolomiets and J.-M. Lehn, *Chem. Commun.*, 2005, 1519–1521.
9 W. H. Binder, S. Bernstorff, C. Kluger, L. Petraru and M. J. Kunz, *Adv. Mater.*, 2005, **17**, 2824–2828.
10 R. Schmidt, M. Stolte, M. Grüne and F. Würthner, *Macromolecules*, 2011, **44**, 3766–3776.
11 P. S. Corbin, L. J. Lawless, Z.-T. Li, Y. Ma, M. J. Witmer and S. C. Zimmerman, *PNAS*, 2002, **99**, 5099–5104.
12 R. P. Sijbesma, F. H. Beijer, L. Brunsveld, B. J. B. Folmer, J. H. K. Ky Hirschberg, R. F. M. Lange, J. K. L. Lowe and E. W. Meijer, *Science*, 1997, **278**, 1601–1604.
13 F. H. Beijer, R. P. Sijbesma, H. Kooijman, A. L. Spek and E. W. Meijer, *J. Am. Chem. Soc.*, 1998, **120**, 6761–6769.
14 (*a*) V. G. H. Lafitte, A. E. Aliev, P. N. Horton, M. B. Hursthouse, K. Bala, P. Golding and H. C. Hailes, *J. Am. Chem. Soc.*, 2006, **128**, 6544–6545; (*b*) K. Bala, H. C. Hailes, V. G. H. Lafitte, A. Aliev and P. Golding, WO 2007/072000 A1, June 2007.
15 E. Greco, A. E. Aliev, V. G. H. Lafitte, K. Bala, D. Duncan, L. Pilon, P. Golding and H. C. Hailes, *New J. Chem.*, 2010, **34**, 2634–2642.
16 C. C. Cheng, C. F. Huang, Y. C. Yen and F. C. Chang, *J. Polym. Sci., Part A: Polym. Chem.*, 2008, **46**, 6416–6424.
17 Y. S. Wang, C. C. Cheng, Y. S. Ye, Y. C. Yen and F. C. Chang, *ACS Macro Lett.*, 2012, **1**, 159–162.
18 I. H. Lin, C. C. Cheng, Y. C. Yen and F. C. Chang, *Macromolecules*, 2010, **43**, 1245–1252.
19 Y. C. Yen, C. C. Cheng, Y. L. Chu and F. C. Chang, *Polym. Chem.*, 2011, **2**, 1648–1653.
20 C. C. Cheng, Y. L. Chu, P. H. Huang, Y. C. Yen, C. W. Chu, A. C. M. Yang, F. H. Kuo, J. K. Chen and F. C. Chang, *J. Mater. Chem.*, 2012, **22**, 18127–18131.
21 Y. L. Chu, C. C. Cheng, Y. C. Yen and F. C. Chang, *Adv. Mater.*, 2012, **24**, 1894–1898.
22 C. C. Cheng, Y. L. Chu, F. C. Chang, D. J. Lee, Y. C. Yen, J. K. Chen, C. W. Chu and Z. Xin, *Nano Energy*, 2015, **13**, 1–8.
23 (*a*) G. Ercolani, L. Mandolini, P. Mencarelli and S. Roelens, *J. Am. Chem. Soc.*, 1993, **115**, 3901–3908; (*b*) C. A. Hunter and H. L. Anderson, *Angew. Chem., Int. Ed.*, 2009, **48**, 7488–7499; (*c*) T. Haino, A. Watanabe, T. Hirao and T. Ikeda, *Angew. Chem., Int. Ed.*, 2012, **51**, 1473–1476.
24 D. Chun, F. Wudl and A. Nelson, *Macromolecules*, 2007, **40**, 1782–1785.
25 (*a*) O. A. Scherman, G. B. W. L. Ligthart, R. P. Sijbesma and E. W. Meijer, *Angew. Chem., Int. Ed.*, 2006, **45**, 2072–2076; (*b*) N. E. Botterhuis, D. J. M. van Beek, G. M. L. van Gemert, A. W. Bosman and R. P. Sijbesma, *J. Polym. Sci., Part A: Polym. Chem.*, 2008, **46**, 3877–3885; (*c*) C. C. Cheng, I. H. Lin, Y. C. Yen, C. W. Chu, F. H. Ko, X. L. Wang and F. C. Chang, *RSC Adv.*, 2012, **2**, 9952–9957.
26 P. Y. W. Dankers, Z. Zhang, E. Wisse, D. W. Grijpma, R. P. Sijbesma, J. Feijen and E. W. Meijer, *Macromolecules*, 2006, **39**, 8763–8771.

 

27 O. Uzun, A. Sanyal, H. Nakade, R. J. Thibault and V. M. Rotello, *J. Am. Chem. Soc.*, 2004, **126**, 14773–14777.
28 T. Shimizu, R. Iwaura, M. Masuda, T. Hanada and K. Yase, *J. Am. Chem. Soc.*, 2001, **123**, 5947–5955.
29 J. Miao and L. Zhu, *Chem. Mater.*, 2010, **22**, 197–206.
30 C. A. Hunter, K. R. Lawson, J. Perkins and C. J. Urch, *J. Chem. Soc., Perkin Trans. 2*, 2001, 651–669.
31 R. Ziessel, G. Pickaert, F. Camerel, B. Donnio, D. Guillon, M. Cesario and T. Prange, *J. Am. Chem. Soc.*, 2004, **126**, 12403–12413.
32 (*a*) P. Rangarajan, R. A. Register, D. H. Adamson, L. J. Fetters, W. Bras, S. Naylor and A. J. Ryan, *Macromolecules*, 1995, **28**, 1422–1428; (*b*) D. J. Quiram, R. A. Register, G. R. Marchand and A. J. Ryan, *Macromolecules*, 1997, **30**, 8338–8343; (*c*) W. P. J. Appel, G. Portale, E. Wisse, P. Y. W. Dankers and E. W. Meijer, *Macromolecules*, 2011, **44**, 6776–6784; (*d*) A. J. P. Teunissen, M. M. L. Nieuwenhuizen, F. Rodríguez-Llansola, A. R. A. Palmans and E. W. Meijer, *Macromolecules*, 2014, **47**, 8429–8436.